Serialized Stepwise Parameter Calibration Strategy for a Compact Transient Switching Model of PCMO RRAM

Vivek Saraswat
Department of Electrical Engineering
Indian Institute of Technology Bombay
Mumbai, India
vsaraswat009@gmail.com

Arpan De
Department of Electronics and Telecommunication Engineering
Jadavpur University
Kolkata, India
arpantukan@gmail.com

Jayatika Sakhuja
Department of Electrical Engineering
Indian Institute of Technology Bombay
Mumbai, India
18307r013@iitb.ac.in

Udayan Ganguly
Department of Electrical Engineering
Indian Institute of Technology Bombay
IITB Centre for Semiconductor Technologies (SemiX)
Mumbai, India
udayan@ee.iitb.ac.in

***Abstract*—PCMO RRAM, a type of non-filamentary bulk switching RRAM demonstrates complex switching transients from fast (ns) to long (s) time range. A reaction-drift phenomena with self-heating-based switching model has been proposed earlier, along with space charge-limited carrier conduction from TCAD. In this work, a complete and circuit-ready conduction + switching model in Verilog-A has been proposed using shallow trap assumption based analytical solution. Further, a stepwise method to uniquely calculate the physical parameters of the multiple equations involved in the self-consistent solution is proposed for the Set and Reset processes. The obtained parameters agree well with the parameters reported using electrical or material characterization.**

Keywords—PCMO, RRAM, Verilog-A, compact modelling, calibration, parameters

I. INTRODUCTION

$Pr_{1-x}Ca_xMnO_3$ (PCMO)-based RRAM is a type of non-filamentary, bipolar RRAM which exhibits current scaling and low variability [1], [2]. It demonstrates versatile applications from analog neuromorphic synapses [3], to stochastic neurons [4]. Well-calibrated physics-based models are crucial for predicting performance of fabricated structures and enabling large-scale circuit level applications. A "TCAD+Matlab" hybrid model was proposed with oxygen vacancies-based trap-modulated space charge limited conduction (in TCAD), thermal dynamics due to self-heating and reaction-drift ion dynamics for resistive switching (in MATLAB) [5]. The model captured the complex Set and Reset transients over many orders of timescales (100 ns - 1 s). Under the assumption of shallow traps being dominant for conduction, a compact expression for the carrier conduction can be derived to eliminate the dependence on TCAD [6]. Here, a circuit-ready and compact model for PCMO RRAM switching transients implemented in Verilog-A is presented. However, self-consistent solution to multiple physical models like carrier conduction, thermal and ion dynamics presents a significant challenge to uniquely calibrating the model parameters. The challenge is exacerbated in the presence of new materials with limited electrical characterization data. Here, we present a stepwise manner to extract model parameters uniquely and compare extracted parameters to reported values to demonstrate promising agreement.

This work is supported in parts by the Department of Science and Technology (DST) Nano Mission, Ministry of Electronics, and IT (MeitY) and Department of Electronics through the Nanoelectronics Network for Research and Applications (NNETRA) project, Govt. of India. Vivek Saraswat and Jayatika Sakhuja are supported by Prime Minister's Research Fellowship, Govt. of India.

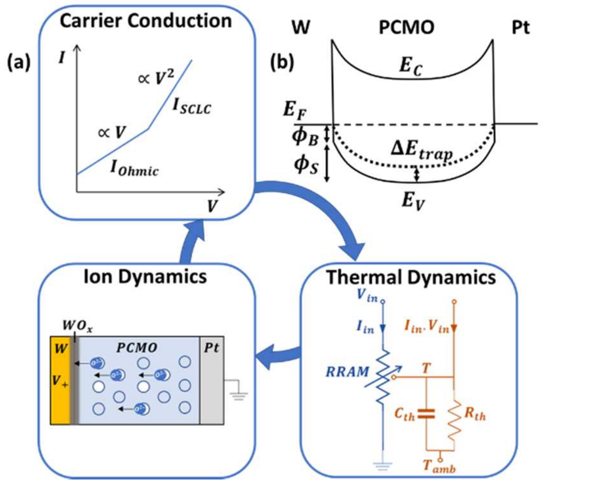

Fig. 1. (a) Self-consistent solution between carrier conduction, thermal dynamics, and ion dynamics for PCMO RRAM transient switching model, (b) Equilibrium band diagram showing the barriers and shallow trap level in the Ohmic conduction limit

II. EXPERIMENTAL SECTION

PCMO-based RRAM has a $Si/SiO_2/Ti/Pt/PCMO/W$ stack. PCMO (60 nm) is sandwiched between a noble bottom (Pt) and a reactive top (W) electrode. PCMO is deposited by RF sputtering followed by O_2 annealing. Top W pads of side 5 μm are patterned by photolithography and lift-off [7]. All DC IV measurements are performed using Source Measurement Unit (SMU) and all transient measurements are performed using Waveform Generator / Fast Measurement Unit (WGFMU) – B1500/1530A.

III. VERILOG-A COMPACT MODEL

The transient resistive switching current in PCMO RRAM can be modelled by the self-consistent solution to Ohmic+Space Charge Limited Conduction (SCLC), self-heating and reaction-drift of ions in the presence of field and temperature to modulate oxygen vacancy-based trap density (Fig. 1. (a)). Ohmic current calculation requires calculation of band-bending (ϕ_S) due to trapped charges which can be solved analytically under the assumption of shallow traps ($\Delta E_{trap} \ll E_F - E_V$) (Fig. 1. (b)) [6]. The trap-SCLC current can be calculated as a function of an N_T dependent factor (θ) and trap-free SCLC current. The Ohmic and SCLC current equations are as follows:

$$J_{total} = J_{Ohmic} + J_{SCLC} \quad (1)$$

$$J_{Ohmic} = q\mu p \frac{V}{L} \quad (2)$$

$$p = N_V \exp\left(-\frac{\phi_S+\phi_B}{k_B T}\right) \quad (3)$$

$$N_V = N_{V,300}\left(\frac{T}{300}\right)^{3/2} \quad (4)$$

$$\phi_S = k_B T \ln\left(\frac{q^2L^2(\theta+1)}{2\pi^2 \varepsilon k_B T} N_T \exp\left(\frac{\Delta E_{trap}}{k_B T}\right)\right) \quad (5)$$

$$\Rightarrow p = \frac{2\pi^2 \varepsilon k_B T}{q^2 L^2} \frac{\theta}{\theta+1} \exp\left(-\frac{\phi_B}{k_B T}\right) \quad (6)$$

$$J_{SCLC} = \frac{\theta}{\theta+1} J_{free} \quad (7)$$

$$\theta = \frac{N_V}{N_T} \exp\left(-\frac{\Delta E_{trap}}{k_B T}\right) \quad (8)$$

$$J_{free} = \frac{9}{8}\mu\varepsilon \frac{V^2}{L^3} \quad (9)$$

The self-heating dynamics can be modelled simply as a thermal RC circuit dissipating electrical power through the device:

$$C_{th}\frac{dT}{dt} = I.V - \frac{T-T_{amb}}{R_{th}} \quad (10)$$

The ion dynamics requires consideration of reaction at the W interface to capture oxygen and generate vacancies that can then drift into the bulk activated by field and temperature, increasing the bulk trap density for Reset (and vice-a-versa for Set) [5]:

$$\frac{dN_T}{dt} = \pm \frac{n k_r}{L (N_T)^n} v_{drift} \quad (11)$$

$$v_{drift} = af \exp\left(-\frac{E_a}{k_B T}\right) \sinh\left(\frac{V/L}{\xi_0}\right) \quad (12)$$

$$\xi_0 = \frac{2k_B T}{qa} \quad (13)$$

IV. Calibration Strategy

The effective list of parameters that can be calibrated from electrical measurements is shown in Table I. If the assumed parameters are changed, this will result in changing the calibrated parameters without affecting the calibration strategy or the quality of calibration.

A. Set Calibration

1) In order to find the mobility (μ), we observe the first DC IV sweep of PCMO RRAM, i.e., the virgin low resistance state (LRS) (Fig. 2. (a)). The exponent shows as current goes from Ohmic to SCLC to self-heating limited followed by resistive switching regimes (Fig. 2. (b)). Mobility controls the trap-free SCLC current. 2) Calibration of Ohmic region current on the other hand is controlled by the valence band offset (ϕ_B). We next observe the transient Set currents at different Set voltages ($|V_{Set}|$) (Fig. 2. (c)). Using a t_{settle}, we can extract the initial settling current I_{settle} at different voltages. 3) I_{settle} at low voltages is calibrated by the choice of the starting trap density (N_{T0}) in the model (Fig. 2. (d)). 4) Next, the slope of I_{settle} vs. $|V_{Set}|$ is calibrated using the thermal resistance (R_{th}) (Fig. 2. (e)).

TABLE I. Parameters of the Compact Model

Effective List of Parameters Needing Calibration		
μ	Mobility	?
ϕ_B	Valence Band Offset	
N_T	Trap Density	
R_{th}	Thermal Resistance	
C_{th}	Thermal Capacitance	
k_r	Reaction Constant	
a	Characteristic Field Length	
E_a	Activation Energy for Ion Migration	
Assumed/Known Parameters		
N_V	Valence Band Density of States	$10^{19}\ cm^{-3}$
ΔE_{trap}	Trap Energy from Valence Band	$80\ mV$
ε	Dielectric Constant	$30\ \varepsilon_0$
n	Traps per ion	2
L	Film Thickness	$60\ nm$
f	Migration Frequency	$10^{13}\ Hz$
A	Electrode Area	$(5\ \mu m)^2$

From the transient Set currents, using a fixed target I_{Set}, we can extract the t_{Set}, i.e., the time to Set at different $|V_{Set}|$. The modelled temperatures at settling currents reveal a field-activated (low voltage) and a temperature activated (high voltage) ionic drift region (Fig. 2. (f)). 5) and 6) The slope of t_{Set} vs. $|V_{Set}|$ can be calibrated using the characteristic field at room temperature (a) in the first region and the ion migration activation energy (E_a) for the second region. 7) After calibrating the slopes, the reaction constant (k_r) is used to match the absolute levels of observed t_{Set} values. 8) Finally, the C_{th} calibrates the saturation timescale for t_{Set} at high voltages. The simulated Set transients for the experimental range of $|V_{Set}|$ shows excellent match with experiments (Fig. 2. (g) and (c)).

A. Reset Calibration

For the Reset transients, the currents approach a universal time slope of -1/10 (Fig. 3. (a)). 1) With an initial trap density (N_{T0}) that dictates the initial rise in current, the gradual fall in current is controlled by the response of v_{drift} to falling current and hence the falling temperature (Fig. 3. (b)). 2) This universal slope is calibrated by the temperature activated E_a for the Reset case. 3) Next, k_r ensures that the time of merger of the current falling with universal slope to the rest of the transient can be calibrated correctly (Fig. 3. (b)). 4) Finally, R_{th} controls the excess heating that happens at higher voltages thus resulting in a sharp initial drop in current (Fig. 3. (b)). The simulated Reset transients show excellent match with the experimental Reset transients (Fig. 3. (c)). The list of calibrated parameters is shown in Table II. alongside previously reported values to show good agreement.

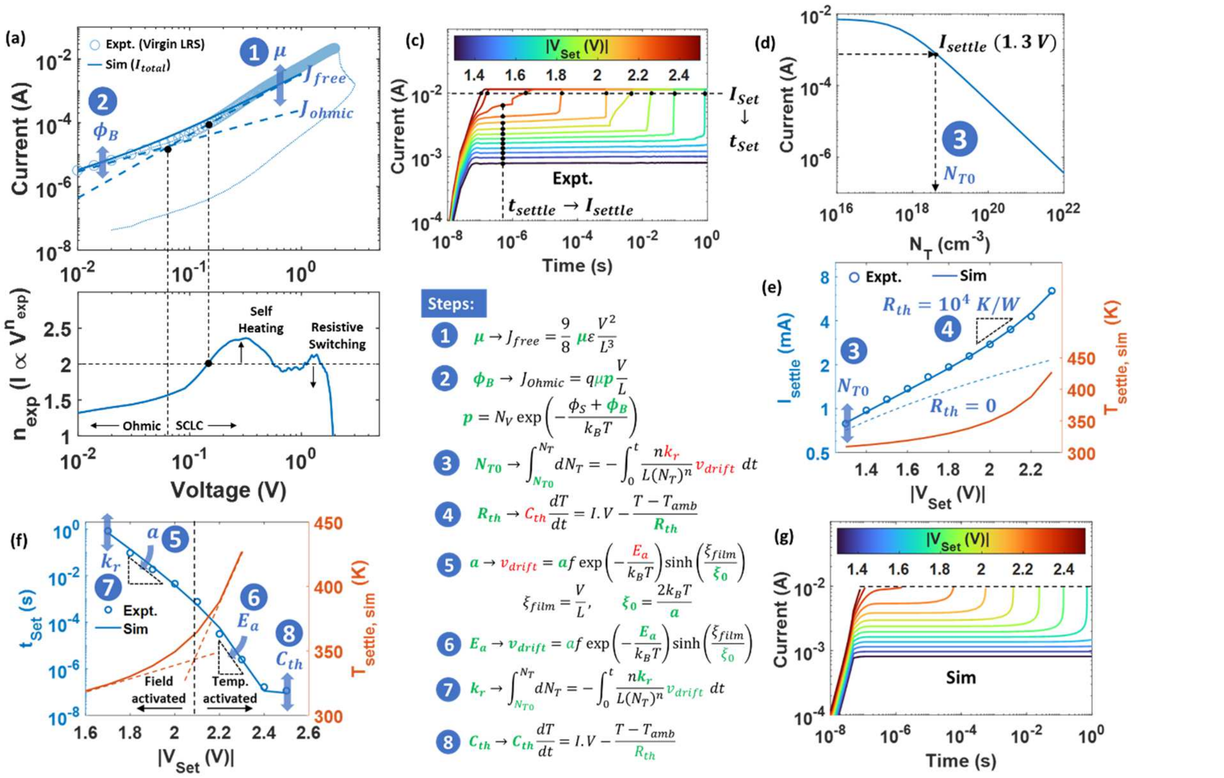

Fig. 2. Calibration strategy for Set: (a) Virgin LRS DC IV to capture μ and ϕ_B, (b) Exponent of Virgin LRS DC IV to highlight Ohmic, SCLC, self-heating, and resistive switching regions, (c) Experimental Set Transients, extraction of I_{settle} and t_{Set}, (d) Modelled current vs. trap-density at 1.3 V, extraction of N_{T0}, (e) Extraction of R_{th} from I_{settle} vs. $|V_{Set}|$ and modelled T_{settle}, (f) Extraction of a, E_a k_r and C_{th} from field-activated and temperature activated regions of t_{Set} vs. $|V_{Set}|$, (g) Calibrated Set transients from model

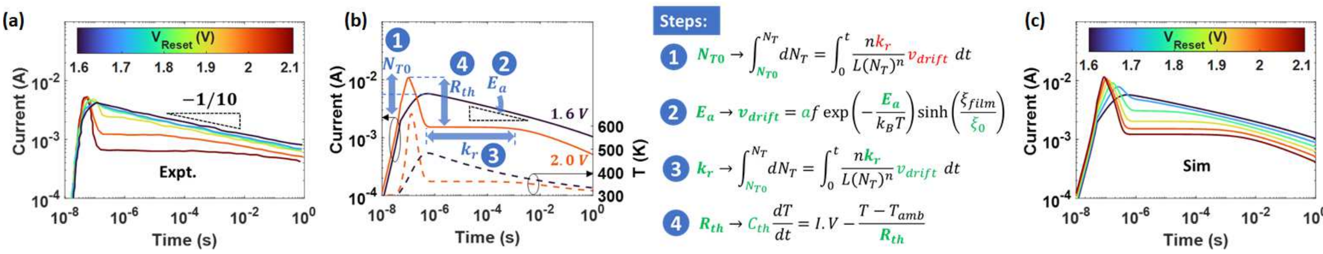

Fig. 3. Calibration strategy for Reset: (a) Experimental Reset Transients demonstrating universal slope, (b) Extraction of N_{T0}, E_a, k_r and R_{th} from low and high bias modelled currents to get required universal slope and current separation along with modelled $T(t)$, (c) Calibrated Reset Transients from model

V. Conclusion

We present a compact Verilog-A model for switching transients in PCMO RRAM. The model consists of 8 independently tunable parameters across a variety of physics like carrier conduction, thermal and reaction constants and ionic transport. We present a stepwise calibration strategy to uniquely calculate the model parameters ensuring that each step requires the tuning of only one parameter at a time which is highly efficient compared to higher dimensional sweeping calibration or machine learning calibration strategies. Moreover, the calibration depends only on DC and transient electrical characterization data thus highlighting a powerful method of extracting material parameters using the complex RRAM switching behaviors.

TABLE II. Calibrated Parameters

Parameters		Calibrated Values		Reported Values
		Set	Reset	
μ (cm^2/V-s)		1.3		0.01 – 1 [8]
ϕ_B (meV)		50		-
N_T (cm^{-3})	Range	$10^{16} - 10^{21}$		-
	N_{T0}	5×10^{18}	3×10^{18}	-
R_{th} (K/W)		1×10^4	2×10^4	$0.5 - 1 \times 10^4$ *[9]
C_{th} (pJ/K)		1.5		~ 3 *[10]
k_r ($\times \mu m^{-3}$)^3		4.6×10^{-4}	6.5×10^{-2}	-
a (nm)		40		-
E_a (eV)		1.1	1.5	0.8 – 1.6 [11]

*Effective values extracted for stack from material thermal conductivities and capacities

References

[1] P. Kumbhare, I. Chakraborty, A. Khanna, and U. Ganguly, "Memory Performance of a Simple Pr 0.7 Ca 0.3 MnO 3 -Based Selectorless RRAM," *IEEE Trans. Electron Devices*, vol. 64, no. 9, pp. 3967–3970, Sep. 2017, doi: 10.1109/TED.2017.2725900.

[2] N. Panwar and U. Ganguly, "Variability assessment and mitigation by predictive programming in Pr0.7Ca0.3MnO3 based RRAM," in *2015 73rd Annual Device Research Conference (DRC)*, IEEE, Jun. 2015, pp. 141–142. doi: 10.1109/DRC.2015.7175595.

[3] K. Moon *et al.*, "Bidirectional non-filamentary RRAM as an analog neuromorphic synapse, Part I: Al/Mo/Pr0.7Ca0.3MnO3 material improvements and device measurements," *IEEE J. Electron Devices Soc.*, vol. 6, no. 1, pp. 146–155, 2018, doi: 10.1109/JEDS.2017.2780275.

[4] D. Khilwani *et al.*, "PrxCa1−xMnO3 based stochastic neuron for Boltzmann machine to solve 'maximum cut' problem," *APL Mater.*, vol. 7, no. 9, p. 091112, Sep. 2019, doi: 10.1063/1.5108694.

[5] V. Saraswat *et al.*, "Reaction-Drift Model for Switching Transients in $Pr_{0.7}Ca_{0.3}MnO_3$-Based Resistive RAM," *IEEE Trans. Electron Devices*, vol. 67, no. 9, pp. 3610–3617, Sep. 2020, doi: 10.1109/TED.2020.3011387.

[6] I. Chakraborty, A. K. Singh, P. Kumbhare, N. Panwar, and U. Ganguly, "Materials parameter extraction using analytical models in PCMO based RRAM," in *2015 73rd Annual Device Research Conference (DRC)*, IEEE, Jun. 2015, pp. 87–88. doi: 10.1109/DRC.2015.7175568.

[7] S. Chouhan, P. Kumbhare, A. Khanna, N. Panwar, and U. Ganguly, "Effect of thermal resistance and scaling on dc-IV characteristics of PCMO based RRAM devices," in *2017 75th Annual Device Research Conference (DRC)*, IEEE, Jun. 2017, pp. 1–2. doi: 10.1109/DRC.2017.7999428.

[8] B. Ifland *et al.*, "Current–voltage characteristics of manganite–titanite perovskite junctions," *Beilstein J. Nanotechnol.*, vol. 6, pp. 1467–1484, Jul. 2015, doi: 10.3762/bjnano.6.152.

[9] I. Chakraborty, N. Panwar, A. Khanna, and U. Ganguly, "Space Charge Limited Current with Self-heating in $Pr_{0.7}Ca_{0.3}MnO_3$ based RRAM," May 2016, [Online]. Available: http://arxiv.org/abs/1605.08755

[10] N. Panwar, A. Khanna, P. Kumbhare, I. Chakraborty, and U. Ganguly, "Self-Heating during submicrosecond Current Transients in Pr0.7Ca0.3MnO3-Based RRAM," *IEEE Trans. Electron Devices*, vol. 64, no. 1, pp. 137–144, 2017, doi: 10.1109/TED.2016.2632712.

[11] P. Kumbhare and U. Ganguly, "Ionic Transport Barrier Tuning by Composition in Pr 1–x Ca x MnO 3 -Based Selector-Less RRAM and Its Effect on Memory Performance," *IEEE Trans. Electron Devices*, vol. 65, no. 6, pp. 2479–2484, Jun. 2018, doi: 10.1109/TED.2018.2827420.